

# Excited-state quantum phase transition and the quantum speed limit

Qian Wang<sup>1</sup>

<sup>1</sup>*Department of Physics, Zhejiang Normal University, Jinhua 321004, China*

Francisco Pérez-Bernal<sup>2</sup>

<sup>2</sup>*Dep. CC. Integradas y Centro de Estudios Avanzados en Física, Matemáticas y Computación. Fac. CC. Experimentales, Universidad de Huelva, Huelva 21071, Spain*

(Dated: October 21, 2019)

We investigate the influence of an excited-state quantum phase transition (ESQPT) on the quantum speed limit (QSL) time of an open quantum system. The system consists of a central qubit coupled to a spin environment modeled by a Lipkin-Meshkov-Glick (LMG) Hamiltonian. We show that when the coupling between qubit and environment is such that the latter is located at the ESQPT critical energy the qubit evolution shows a remarkable slowdown, marked by an abrupt peak in the QSL time. Interestingly, this slowdown at the ESQPT critical point is induced by the singular behavior of the qubit decoherence rate, being independent of the Markovian nature of the environment.

## I. INTRODUCTION

Quantum phase transitions (QPTs) are zero-temperature phase transitions in which system ground state undergoes a qualitative variation once a Hamiltonian control parameter (such as an internal coupling constant or an external field strength) reaches a critical value. QPTs are non-thermal and driven by quantum fluctuations in a many-body quantum system [1–3]. They are the best known example of criticality in quantum mechanics and, in the past decades, theoretical [4–9] and experimental [10–12] groups have paid much attention to this subject. Nowadays QPTs are considered a keynote topic in many fields of quantum physics. In particular, ground state QPTs between different geometrical limits of algebraic models applied to nuclear and molecular structure have been extensively studied [13–17].

More recently, it has been found that the QPT concept, originally defined considering the system ground state, can be generalized and extended to the realm of excited states [18–20]. Such excited-state quantum phase transitions (ESQPTs) are marked by a discontinuity in the density of excited states at a critical value of the energy of the system. Such discontinuity, occurring at values of the control parameter other than the critical one, is a continuation at higher energies of the level clustering near the ground state energy that characterizes the ground state QPT [20–23]. Establishing a parallelism with the Ehrenfest classification for ground state QPTs, ESQPTs can also be characterized by the nonanalytic evolution of the energy of an individual excited state of the system when varying the control parameter [20, 24–26].

During the last decade, ESQPTs have been theoretically analyzed in various quantum many-body systems: the Lipkin-Meshkov-Glick (LMG) model [16, 22], the vibron model [20, 25], the interacting boson model [27], the kicked-top model [28], and the Dicke model [26, 29–31] among others. Furthermore, the existence of a relation between ESQPTs and the onset of chaos has been

explored in Ref. [29] and ESQPT signatures have been experimentally observed in superconducting microwave billiards [32], different molecular systems [33, 34], and spinor Bose-Einstein condensates [35]. The ESQPT influence on the dynamics of quantum systems has recently attracted significant attention and several remarkable dynamical effects of ESQPTs have been revealed [22, 24, 26, 36–43]. In particular, the impact of ESQPTs on the adiabatic dynamics of a quantum system has been recently analyzed [44], as well as the relationship between thermal phase transitions and ESQPTs [45].

On the other hand, due to fast progresses in the fields of quantum computation and quantum information science, the quantum speed limit (QSL) is in the limelight and its study has drawn considerable attention in isolated (see Refs. [46, 47] and references therein) and open [48–56] quantum systems. The QSL is characterized by the QSL time, which is defined as the minimum evolution time required by a quantum system to evolve between two distinct states [47, 48, 57]. Nowadays the QSL plays an important role in many areas of quantum physics, see e.g. the recent review in Ref. [46] and references therein. Interestingly, there is a common belief that the QSL is a strictly quantum phenomenon, without a classical counterpart. However, speed limit bounds in classical systems in close connection with the QSL have been recently reported [58, 59].

For open quantum systems, one can expect that the QSL should be strongly influenced by decoherence effects that stem from the interaction between the system and the environment. It has already been shown that the system decoherence can be enhanced by quantum criticality in the environment [6, 24]. Hence, one would naturally expect a connection between the occurrence of a QPT in the environment and a variation in the QSL time. Indeed, recent results obtained for open systems consisting of a qubit coupled to a spin  $\frac{1}{2}$  XY chain with nearest neighbors interaction [60] or to a LMG bath [61] clearly verify that the QSL time has a remarkable variation in the critical point of the environment ground state QPT.

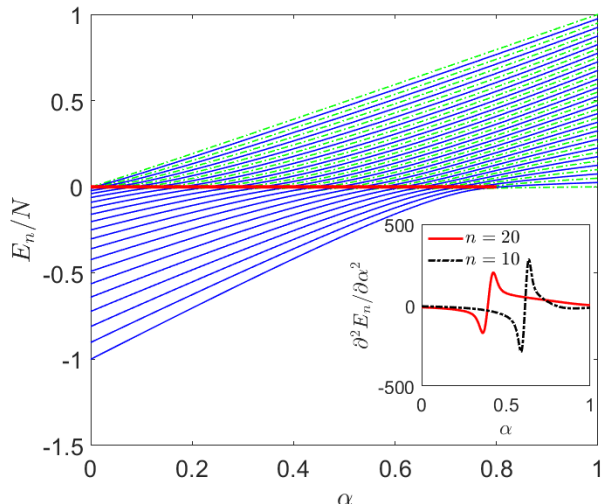


FIG. 1. Energy levels of the environment Hamiltonian (3) as a function of the control parameter  $\alpha$  with  $N = 40$ . Odd(Even)-parity levels are depicted with blue solid (green dotted dashed) curves. The thick red line indicates the critical energy  $E_c = 0$  of the ESQPT. Inset: the second derivative of the level energy with respect to the variable  $\alpha$  for the 10th and 20th excited states, respectively.

This happens to such extent that the QSL time has been proposed as a possible probe to detect the occurrence of ground state QPTs [60, 61].

In this work, we extend the results obtained for ground state QPTs in [60, 61] toward excited states and ESQPTs, to uncover the relationship between criticality in ESQPTs and the QSL. With this aim, we analyze the QSL time of an open system that consists of a central qubit coupled to a LMG bath [62]. The variation of the coupling strength between the qubit and the environment can drive the environment through the critical point of an ESQPT and we report the effects that the crossing has on the QSL time. Moreover, since the Markovian nature of the environment has a strong influence on the properties of the QSL, we will also study the ESQPT effects on the environment's Markovian nature in order to get a deeper understanding on the relationship between ESQPTs and the QSL.

The remainder of this article is organized as follows. In Sec. II, we introduce the model and analyze the phase-transitional properties of the environment, especially those related to ESQPTs. In Sec. III we report the QSL time for the qubit and investigate how the ESQPT affects the behavior of the QSL time. In Sec. IV we offer a physical explanation for the singular behavior of the QSL time at the critical point of the ESQPT. We also discuss in this section how the variation of the QSL time at the ESQPT critical point stems from the singular behavior of the qubit decoherence rate instead of from the Markovian nature of the environment. Finally, we discuss and summarize our results in Sec. V.

## II. MODEL

We consider a system composed by a qubit coupled to a spin environment. The Hamiltonian of the total system is [6, 22, 63]

$$\hat{H} = \hat{H}_{\mathcal{E}} + \hat{H}_{S\mathcal{E}}, \quad (1)$$

where  $\hat{H}_{\mathcal{E}}$  is the environment Hamiltonian and the interaction between qubit and environment is modeled by  $\hat{H}_{S\mathcal{E}}$ , which can be written as [22, 24]

$$\hat{H}_{S\mathcal{E}} = |0\rangle\langle 0| \otimes \hat{H}_0 + |1\rangle\langle 1| \otimes \hat{H}_1, \quad (2)$$

where,  $|0\rangle$  and  $|1\rangle$  denote the two components of the qubit, while  $\hat{H}_0$  and  $\hat{H}_1$  are interaction Hamiltonians that act upon the environment Hilbert space. Therefore, depending on the particular qubit state, the environment evolution takes place under a different effective Hamiltonian  $\hat{H}_{\mathcal{E}}^l = \hat{H}_{\mathcal{E}} + \hat{H}_l$  with  $l = 0, 1$ . By changing the interaction Hamiltonian  $\hat{H}_l$ , one can drive the environment through its critical point [22, 24].

Specifically, the environment in our study is given by the generalized LMG model. This model, originally introduced as a toy model in Nuclear structure to test the validity of different approximations [62], has been recently extensively used to study ESQPTs [22, 24, 37, 64] and has been implemented in the laboratory making use of different platforms: trapped ions [65], Bose-Einstein condensates [66, 67], and optical cavities [68]. The LMG model Hamiltonian is

$$\hat{H}_{\mathcal{E}} = -\frac{4(1-\alpha)}{N} \hat{S}_x^2 + \alpha \left( \hat{S}_z + \frac{N}{2} \right), \quad (3)$$

where  $N$  is the size of the environment, the control parameter  $0 \leq \alpha \leq 1$  denotes the strength of the magnetic field along the  $z$  direction, and  $S_\gamma = \sum_{j=1}^N \sigma_\gamma^j$ , the sum of Pauli spin matrices  $\sigma_\gamma$  for  $\gamma = \{x, y, z\}$ . The Schwinger transformation allows to recast Hamiltonian (3) in terms of two scalar creation (and annihilation) bosonic operators  $t^\dagger$  and  $s^\dagger$  ( $t$  and  $s$ ) as follows

$$\hat{H}_{\mathcal{E}} = \alpha \hat{n}_t - \frac{1-\alpha}{N} \hat{Q}^2, \quad (4)$$

where  $\hat{n}_t = t^\dagger t$  and  $\hat{Q} = t^\dagger s + s^\dagger t$  [22, 37]. Clearly, the total number of bosons  $\hat{N} = \hat{n}_s + \hat{n}_t = s^\dagger s + t^\dagger t$  is a conserved quantity, i.e.,  $[\hat{N}, \hat{H}_{\mathcal{E}}] = 0$ . We should point out that for simplicity, we consider  $\hbar = 1$  throughout this article and set the quantities in our study as unitless.

The Hamiltonian (3) can be written down in matrix form using the  $|[N]n_t\rangle$  basis [22, 37], associated with a  $U(2) \supset U(1)$  dynamical symmetry [69],

$$|[N]n_t\rangle = \frac{(t^\dagger)^{n_t} (s^\dagger)^{N-n_t}}{\sqrt{(n_t)!(N-n_t)!}} |0\rangle, \quad (5)$$

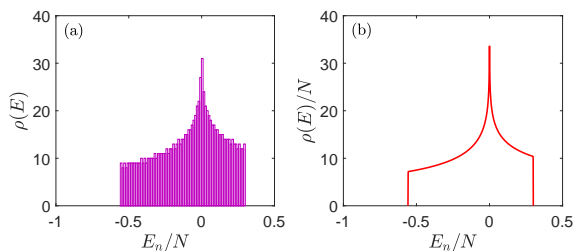


FIG. 2. (a) Density of states of the environment Hamiltonian (3) for  $N = 2000$  with  $\alpha = 0.3$ . (b) Normalized density of states of  $\hat{H}_{\mathcal{E}}$ , calculated by means of Eq. (8), with  $N = 2000$  and  $\alpha = 0.3$ .

where  $|0\rangle = |0_t, 0_s\rangle$  is the vacuum state and  $N \geq n_t \geq 0$ . Obviously, the dimension of the Hamiltonian matrix is  $\text{Dim}[H_{\mathcal{E}}] = N + 1$  and the nonzero matrix elements are

$$\langle N, n_t | H_{\mathcal{E}} | N, n_t \rangle = \alpha n_t + f, \quad (6)$$

$$\langle N, n_t | H_{\mathcal{E}} | N, n_t + 2 \rangle = -\frac{1-\alpha}{N} \sqrt{(n_t+1)(N-n_t)} \times \sqrt{(n_t+2)(N-n_t-1)}, \quad (7)$$

where  $f = -(1-\alpha)/(N)[(n_t+1)(N-n_t)+n_t(N-n_t+1)]$ . The  $\hat{H}_{\mathcal{E}}$  eigenstates and eigenvalues can be obtained through a numerical diagonalization of the corresponding matrix. As the Hamiltonian (3) conserves parity, the parity operator,  $\Pi = (-1)^{n_t}$ , split the Hamiltonian matrix into even- and odd-parity blocks, with dimension  $\text{Dim}[H_{\mathcal{E}}]_{\text{even}} = N/2 + 1$  and  $\text{Dim}[H_{\mathcal{E}}]_{\text{odd}} = N/2$  [37]. In our study, we will consider only the even parity block, which contains the environment ground state. Note that in the thermodynamic limit of Hamiltonian (3) the spectrum of both blocks, even and odd, becomes identical.

### A. Phase transitions in the environment

It is well known that the LMG model Hamiltonian in Eq. (3) exhibits a second-order ground state QPT at a critical value of the control parameter  $\alpha_c = 0.8$  [22, 24, 64]. The phase with  $\alpha > \alpha_c$  is the symmetric phase, while the broken-symmetry phase corresponds to control parameter values  $\alpha < \alpha_c$  [22]. However, besides the ground state QPT, the Hamiltonian (3) also displays an ESQPT and the signatures of the ground state QPT, e.g. the nonanalytical evolution of the ground state as the control parameter of the system is varied, will also be exhibited by excited states for  $\alpha < \alpha_c$ , i.e., in the broken-symmetry phase.

The LMG model correlation energy diagram is shown in Fig. 1, depicting energy levels as a function of the control parameter  $\alpha$  for  $\hat{H}_{\mathcal{E}}$  with  $N = 40$ . In this figure it can be easily noticed how pairs of eigenstates with different parity are degenerate for  $E < 0$ , and nondegenerate when  $E > 0$ . Moreover, the energy gap between adjacent energy levels approaches zero around  $E \approx 0$

in the broken-symmetry phase, where energy levels concentrate around  $E = 0$ , marking the high local energy level density that characterizes ESQPTs. Each excited energy level has an inflection point at  $E \approx 0$  [20] that induces a singular behavior in the second derivative of every individual excited state energy with respect to the control parameter  $\alpha$  (see the inset of Fig. 1) [25]. A true nonanalytic behavior only happens in the large  $N$  limit, also called thermodynamical or mean field limit, but even for systems of finite size ( $N = 40$  in Fig. 1) there are clear precursors of the ESQPT effects, like the behavior of  $\partial^2 E_n / \partial \alpha^2$  for  $n > 0$  [25]. Something similar happens for the ground state energy, the  $n = 0$  case, that shows a discontinuity at the critical value of the control parameter,  $\alpha_c$ . The ESQPT can be crossed in two ways, varying the energy for a fixed parameter value  $\alpha < \alpha_c$  or choosing an excited state and varying the control parameter. It is important to understand that different excited states cross the ESQPT at different values of the control parameter  $\alpha$ , as shown in the inset of Fig. 1.

For a given control parameter value  $\alpha < \alpha_c$ , the piling of energy levels at  $E \approx 0$  that marks the ESQPT will lead, in the large  $N$  limit, to a discontinuity in the density of states (DoS). Indeed, as shown in Fig. 2(a), around  $E = 0$  the DoS  $\rho(E)$  of  $\hat{H}_{\mathcal{E}}$  has a peak for finite  $N$ , which will transform to a logarithmic divergence as  $N \rightarrow \infty$  [20, 70]. Therefore, the critical energy of the environment (3) is  $E_c = 0$  and, in fact, ESQPTs are often characterized by the singular behavior of the DoS occurring at the ESQPT critical energy  $E_c$ , for fixed values of the control parameter [20–23, 37]. The divergence of the DoS at  $E_c = 0$  can be understood using a semiclassical approach or the coherent state approach [20].

In the semiclassical limit the quantum expression for the DoS  $\rho(E) = \sum_j \delta(E - E_j)$  can be decomposed into a smooth and an oscillatory component [71],  $\rho(E) = \bar{\rho}(E) + \tilde{\rho}(E)$ . The smooth part,  $\bar{\rho}(E)$ , is also called the Weyl term and is given by the classical phase space integral, while the oscillatory term,  $\tilde{\rho}(E)$ , originates from the quantum fluctuations and can be expressed as a sum over classical periodic orbits [71]. In the classical limit, the oscillatory part can be omitted [26]. Then the DoS of the environment (3) has following form

$$\rho(E) = \bar{\rho}(E) = \left( \frac{N}{2\pi} \right) \int \delta[E - \mathcal{H}(x, p)] dx dp, \quad (8)$$

where the environment's classical counterpart Hamiltonian  $\mathcal{H}(x, p)$  can be obtained via the coherent or intrinsic state approach [22, 26]. The divergence in the DoS is, therefore, generated from the nonanalytical dependence of the classical phase space volume on the energy. The appearance of such nonanalyticity is usually associated with stationary points of the classical Hamiltonian [23, 26, 72].

In Fig. 2(b), we plot the smooth part of the environment DoS for Hamiltonian (3) as a function of eigenenergies. Note that the DoS has been normalized by the size of the environment. Obviously, the DoS exhibits a cusp

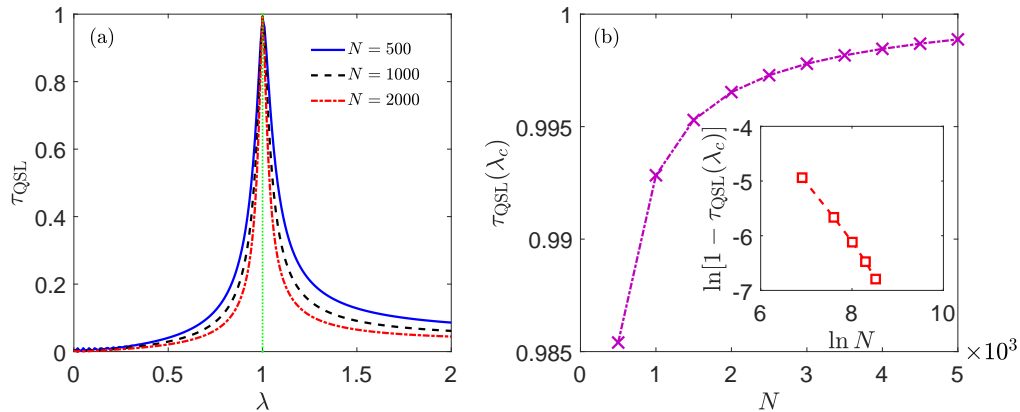


FIG. 3. (a) The QSL time of the qubit as a function of the coupling strength  $\lambda$  for different environment sizes ( $N$  values) for a system with a control parameter  $\alpha = 0.4$ . The actual evolution time is set to unity,  $\tau_e = 1$ . The vertical green dotted line indicates the critical value of the Hamiltonian parameter  $\lambda_c$  obtained for Eq. (12). (b) The critical QSL time  $\tau_{\text{QSL}}(\lambda_c)$  as a function of an environment size  $N$  with  $\alpha = 0.4$  and  $\tau_e = 1$ . Inset:  $1 - \tau_{\text{QSL}}(\lambda_c)$  as a function of  $N$ , in a double logarithmic scale.

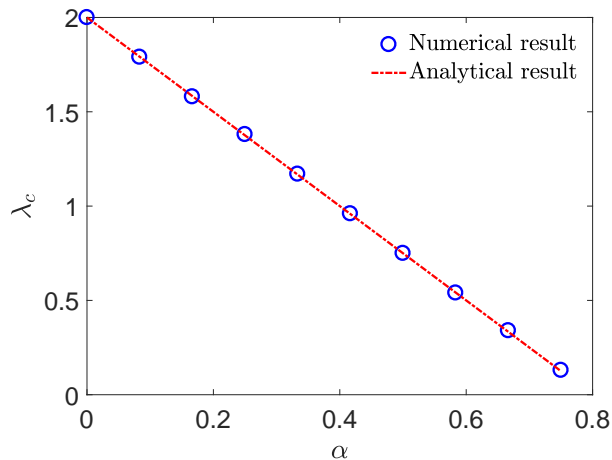


FIG. 4. Critical coupling strength,  $\lambda_c$ , as a function of  $\alpha$  with  $\tau_e = 1$  and an environment size  $N = 1000$ . The numerical result is obtained by identifying the location of the maximum point in  $\tau_{\text{QSL}}$ , while the analytical result is provided by Eq. (12).

singularity (i.e., an infinite peak) at  $E_c = 0$ . Therefore, we confirm that the critical energy of ESQPT is located at  $E_c = 0$ . Moreover, a very good agreement between Figs. 2(a) and 2(b) can be seen clearly.

### B. The critical coupling

In our study the qubit is coupled to the environment (3) with an interaction term

$$\hat{H}_{S\mathcal{E}} = \lambda \sigma_S^z \hat{S}_z, \quad (9)$$

where  $\lambda$  is the coupling strength and  $\sigma_S^z$  is the qubit Pauli matrix. Following Refs. [6, 22], we assume that the qubit is coupled with the environment only in the  $|1\rangle$  state. Therefore, according to Eq. (2), the interaction terms  $\hat{H}_0$  and  $\hat{H}_1$  are given by  $\hat{H}_0 = 0$  and  $\hat{H}_1 = \lambda \hat{S}_z$ , respectively. Making use of the Schwinger transformation, the effective Hamiltonian of the environment has the following expressions [22]

$$\hat{H}_{\mathcal{E}}^0 = -\frac{4(1-\alpha)}{N} \hat{Q}^2 + \alpha \hat{n}_t, \quad (10)$$

$$\hat{H}_{\mathcal{E}}^1 = -\frac{4(1-\alpha)}{N} \hat{Q}^2 + (\alpha + \lambda) \hat{n}_t, \quad (11)$$

when the qubit is in state  $|0\rangle$  and  $|1\rangle$  and where irrelevant constant terms have been omitted.

The variation of the coupling strength  $\lambda$  can drive the environment through the critical point of the ground state QPT. The interplay between the quantum criticality of the environment and the QSL time of the qubit has been analyzed in this way by several works [60, 61] and it has been found that the ground state QPT of the environment substantially diminishes the speed of evolution of the qubit. Our aim in the present work is to assess the effect of the environment ESQPT, instead of the ground state QPT, on the QSL time of the qubit. To this end, we need to know, for a control parameter  $\alpha$  and critical energy  $E_c$ , the value of the coupling parameter—denoted as  $\lambda_c$ —that will take the environment through the ESQPT.

In general, the critical energy of an ESQPT is a function of the control parameter and the value of the critical coupling has to be obtained numerically for any initial state [22, 26]. However, for the LMG bath (3), the critical energy is independent of the control parameter  $\alpha$  as can be seen in Fig. 1. When the initial state of environment is the ground state, the critical value of the coupling

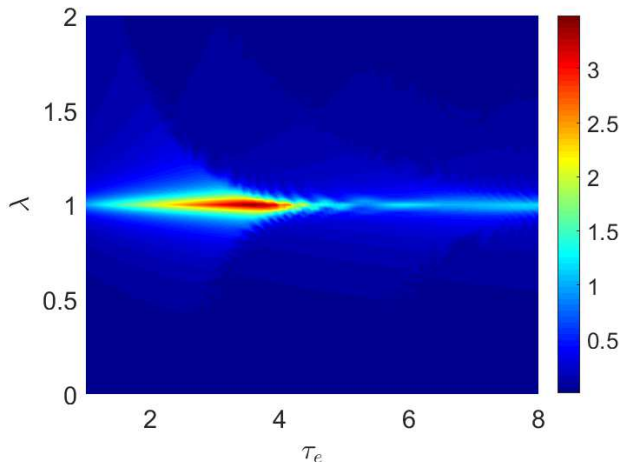


FIG. 5. The QSL time,  $\tau_{\text{QSL}}$ , as a function of the evolution time,  $\tau_e$ , and the coupling strength,  $\lambda$ , with a control parameter  $\alpha = 0.4$  and an environment size  $N = 1000$ .

$\lambda_c$  can be derived using the intrinsic state formalism [24]

$$\lambda_c = 2 - \frac{5}{2}\alpha. \quad (12)$$

We would like to emphasize that the critical coupling  $\lambda_c$ , which induces the ESQPT in the environment Hamiltonian (3), differs from the value  $\lambda_{c0}$  for the ground state QPT [22, 26].

### III. QUANTUM SPEED LIMIT TIME OF THE QUBIT

To understand the effects of the ESQPT on the QSL, we study the QSL time of the qubit after a quench with a coupling strength value such that it drives the environment through the critical energy of the ESQPT. The initial state of the qubit is defined as  $|\psi_0\rangle = \cos(\theta/2)|0\rangle + e^{-i\phi}\sin(\theta/2)|1\rangle$ , while the environment is assumed to be initially in the ground state of  $\hat{H}_{\mathcal{E}}^0$ :  $|\Psi_{\mathcal{E},G}^0\rangle$ . Therefore, the wave function of the total system at  $t = 0$  is  $|\Phi(0)\rangle = [\cos(\theta/2)|0\rangle + e^{-i\phi}\sin(\theta/2)|1\rangle] \otimes |\Psi_{\mathcal{E},G}^0\rangle$ . Evolving the total system wave function according to the Schrödinger equation, the state of the total system at time  $t$  is

$$|\Phi(t)\rangle = \cos(\theta/2)|0\rangle \otimes |\Psi_{\mathcal{E}}^0(t)\rangle + e^{-i\phi}\sin(\theta/2)|1\rangle \otimes |\Psi_{\mathcal{E}}^1(t)\rangle, \quad (13)$$

where the evolution of the environmental states  $|\Psi_{\mathcal{E}}^0(t)\rangle$  and  $|\Psi_{\mathcal{E}}^1(t)\rangle$  satisfies the Schrödinger equation  $i\partial_t|\Psi_{\mathcal{E}}^l(t)\rangle = \hat{H}_{\mathcal{E}}^l|\Psi_{\mathcal{E}}^l(t)\rangle$ , with  $\hat{H}_{\mathcal{E}}^l$  for  $l = 0, 1$  is given by Eqs. (10) and (11), respectively. The evolution of the qubit, therefore, depends on the dynamics of the two environment branches evolving with effective Hamiltonians  $\hat{H}_{\mathcal{E}}^0$  and  $\hat{H}_{\mathcal{E}}^1$ .

From Eq. (13), the evolved reduced density matrix of

the qubit in the  $\{|0\rangle, |1\rangle\}$  basis is

$$\begin{aligned} \rho_S(t) &= \text{Tr}_{\mathcal{E}}|\Phi(t)\rangle\langle\Phi(t)| \\ &= \begin{bmatrix} \cos^2(\theta/2) & \frac{1}{2}e^{-i\phi}\sin(\theta)\mathcal{M}^*(t) \\ \frac{1}{2}e^{i\phi}\sin(\theta)\mathcal{M}(t) & \sin^2(\theta/2) \end{bmatrix}, \end{aligned} \quad (14)$$

where  $\mathcal{M}(t) = \langle\Psi_{\mathcal{E},G}^0|e^{i\hat{H}_{\mathcal{E}}^0 t}e^{-i\hat{H}_{\mathcal{E}}^1 t}|\Psi_{\mathcal{E},G}^0\rangle$  is known as the decoherence factor. The modulus square of  $\mathcal{M}(t)$  is known as the Loschmidt echo (LE), which has been widely studied in many fields (see, e.g., Ref. [73] and references therein). In the present work, we set the energy of the initial state  $|\Psi_{\mathcal{E},G}^0\rangle$  to zero. Then the decoherence factor  $\mathcal{M}(t)$  in Eq. (14) is reduced to

$$\mathcal{M}(t) = \langle\Psi_{\mathcal{E},G}^0|e^{-i\hat{H}_{\mathcal{E}}^1 t}|\Psi_{\mathcal{E},G}^0\rangle, \quad (15)$$

that can be identified with the survival probability of the initial quantum state  $|\Psi_{\mathcal{E},G}^0\rangle$  evolving under the quenched Hamiltonian  $\hat{H}_{\mathcal{E}}^1$ . In the rest of this section we investigate what happens to the QSL time of the qubit when the environment undergoes an ESQPT. We will show how signatures of the ESQPT manifest themselves in the QSL time of the qubit after quenching the coupling strength between qubit and environment in such a way that the environment passes through the critical point of the ESQPT.

The QSL time for a generic quantum open system whose initial state is given by an arbitrary pure state has the following expression [48]

$$\tau_{\text{QSL}} = \max\left\{\frac{1}{\Gamma_{\tau_e}^1}, \frac{1}{\Gamma_{\tau_e}^2}, \frac{1}{\Gamma_{\tau_e}^\infty}\right\} \sin^2[\mathcal{L}(\rho_0, \rho_{\tau_e})], \quad (16)$$

where  $\tau_e$  is the actual evolution time,  $\mathcal{L}(\rho_0, \rho_{\tau_e}) = \arccos\sqrt{\text{tr}(\rho_0\rho_{\tau_e})}$  is the Bures angle between  $\rho_0$  and  $\rho_{\tau_e}$ , and  $\Gamma_{\tau_e}^p = (1/\tau_e)\int_0^{\tau_e} dt\|L_t(\rho_t)\|_p$  where  $L_t$  is the positive generator given by  $\dot{\rho}_t = L_t(\rho_t)$  [48, 74] and  $\|\mathcal{B}\|_p = [\sum_k b_k^p]^{1/p}$  denotes the Schatten  $p$  norm of the operator  $\mathcal{B}$  [48], where  $b_k$  is the  $k$ th singular value of  $\mathcal{B}$  and  $p$  takes the values  $p = 1, 2, \infty$  that correspond with the trace norm, the Hilbert-Schmidt norm, and the operator norm, respectively.

Combining Eqs. (14) and (16), after some algebra, one finally gets the expression of the QSL time for the qubit evolution from  $t = 0$  to  $t = \tau_e$  that can be written as

$$\tau_{\text{QSL}} = \frac{\sin(\theta)\{1 - \Re[\mathcal{M}(\tau_e)]\}}{(1/\tau_e)\int_0^{\tau_e} dt|\partial_t\mathcal{M}(t)|}, \quad (17)$$

where  $\mathcal{M}(t)$  is the decoherence factor in Eq. (15), while  $\Re[\mathcal{M}(\tau_e)]$  denotes the real part of the decoherence factor at  $t = \tau_e$ . Obviously, the QSL time in Eq. (17) depends on the actual evolution time  $\tau_e$  and on the qubit decoherence rate. In the following, without loss of generality, we set  $\theta = \pi/2$ .

We depict in Fig. 3(a) the QSL time of the qubit as a function of the coupling strength  $\lambda$  where, for the sake of simplicity, we set the evolution time  $\tau_e = 1$ . This

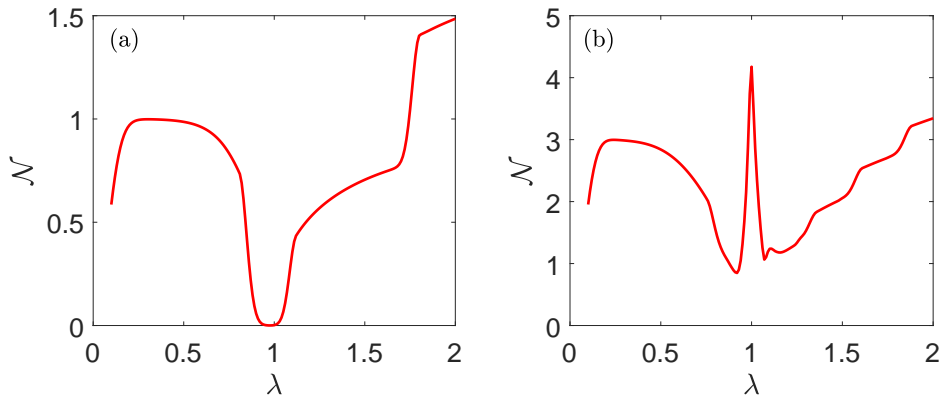


FIG. 6. The non-Markovianity  $\mathcal{N}$  as a function of coupling strength  $\lambda$  for  $\alpha = 0.4$  and environment size  $N = 1000$ , with evolution time values  $\tau_e = 3.5$  (a) and  $\tau_e = 8$  (b).

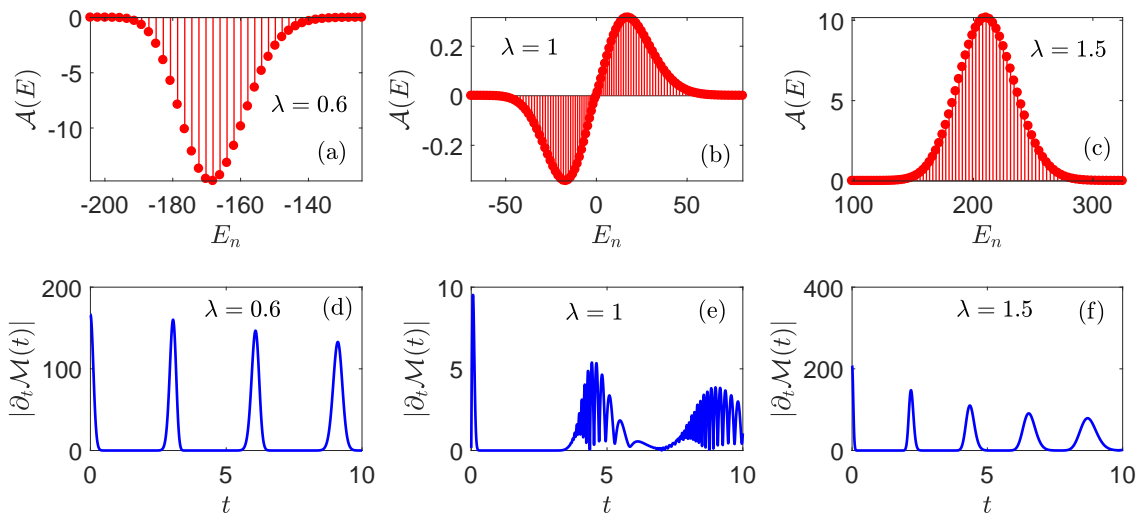


FIG. 7.  $\mathcal{A}(E)$  and  $|\partial_t \mathcal{M}(t)|$  for different coupling strengths for an environment with control parameter  $\alpha = 0.4$  and size  $N = 1000$ . (a)-(c):  $\mathcal{A}(E)$  as a function of  $E_n$  [see Eq. (20)] with  $\lambda$  below (a), at (b), and above (c) the critical coupling strength, respectively. Panels (d)-(f) represent the evolution of  $|\partial_t \mathcal{M}(t)|$  calculated from Eq. (19) for the same coupling parameter values.

figure has several remarkable features. On the one hand, when the value of the coupling strength is far away from the critical value  $\lambda_c$ , the QSL time is small. Moreover, increasing the environment size  $N$ , the evolution of the qubit can be accelerated. On the other hand, it can be clearly noticed in the figure how the QSL time displays a sharp peak at the critical coupling value  $\lambda_c$ , which implies that driving the environment through the ESQPT has as a result a slowdown the quantum evolution of the qubit. The cusplike shape of the QSL time in the vicinity of the critical coupling becomes sharper as the environment size  $N$  increases. Finally, the value of the QSL time at  $\lambda_c$ , i.e., the critical QSL time  $\tau_{\text{QSL}}(\lambda_c)$ , is very close to the actual evolution time and does not depend on the size of environment  $N$ .

In fig. 3(b) we show how the critical QSL time  $\tau_{\text{QSL}}(\lambda_c)$  evolves with the environment size  $N$  for  $\alpha = 0.4$  and  $\tau_e = 1$ . It is obvious that  $\tau_{\text{QSL}}(\lambda_c)$  increases and tends to the actual evolution time for increasing  $N$ . By using the least square method, we find that the relation between  $\tau_{\text{QSL}}(\lambda_c)$  and  $N$  is approximately given as  $1 - \tau_{\text{QSL}}(\lambda_c) = N^{-\mu}$  [cf. the inset of Fig. 3(b)] with  $\mu \approx 1$ . Therefore,  $\tau_{\text{QSL}}(\lambda_c) \rightarrow \tau_e$  in the thermodynamical limit  $N \rightarrow \infty$ .

The features observed in the two panels of Fig. 3 indicate that the QSL time can be used as a proxy for the ESQPT in the environment. To further verify this statement, we compare the numerically estimated critical coupling strength, obtained as the location of the maximum in  $\tau_{\text{QSL}}$ , with the exact value of  $\lambda_c$  in Eq. (12). The results are displayed in Fig. 4 with a very good agreement

between numerical and analytical results, evidencing that the qubit QSL time may be considered a reliable detector of ESQPT in the environment.

The QSL time in Eq. (17) also depends on the evolution time  $\tau_e$  value. Fig. 5 is a heatmap where we display the variation of the QSL time as a function of both  $\tau_e$  and  $\lambda$ , with  $\alpha = 0.4$  and  $\lambda_c = 1$ . This figure has two remarkable features. On the first hand, regardless of the value  $\tau_e$ , the maximum  $\tau_{\text{QSL}}$  value is always reached for the critical coupling strength  $\lambda_c$ . This feature confirms our previous suggestion of the QSL time as a good environment ESQPT indicator. On the second hand, the maximum value of  $\tau_{\text{QSL}}$  exhibits a nonmonotonical behavior for increasing evolution times. This is different from the ground state QPT case, where the extreme value of  $\tau_{\text{QSL}}$  always increases for larger evolution times  $\tau_e$  [60].

#### IV. MECHANISM FOR QUANTUM SLOWDOWN OF THE QUBIT

Both theoretical [48, 75] and experimental [76] studies verified that the Markovian nature of the environment can slow down the quantum evolution of the system. Therefore, we need to investigate if there is any relationship in the increase of the QSL time due to the environment ESQPT and its Markovian nature in order to clarify the origin of the quantum slowdown mechanism at the critical point of ESQPT.

For an open quantum system, the degree of Markovian behavior of the environment can be quantified by the measure of non-Markovianity, defined as [77]

$$\mathcal{N} = \max_{\rho_{1,2}(0)} \int_{\eta > 0} \eta[t, \rho_{1,2}(0)] dt,$$

where the maximization is performed over all initial state pairs  $[\rho_1(0), \rho_2(0)]$  and  $\eta[t, \rho_{1,2}(0)] = d\{D[\rho_1(t), \rho_2(t)]\}/dt$  is the changing rate of the trace distance  $D[\rho_1(t), \rho_2(t)] = \text{Tr}|\rho_1(t) - \rho_2(t)|/2$ , which measures the distinguishability between two time-evolved states  $\rho_{1,2}(t)$  and satisfies  $0 \leq D \leq 1$ . For any operator  $\mathcal{O}$ , the trace norm is defined by  $|\mathcal{O}| = \sqrt{\mathcal{O}^\dagger \mathcal{O}}$ . A Markovian environment is characterized by  $\mathcal{N} = 0$ , while a value  $\mathcal{N} > 0$  indicates an information flow back to the system and, therefore, their non-Markovian character.

It has been found that, for the open system under consideration, the optimal initial state pairs are provided by the antipodal points on the Bloch sphere [78, 79]. Therefore, in our study the measure of non-Markovianity can be calculated as [60]

$$\mathcal{N} = \frac{1}{2} \left[ \int_0^{\tau_e} |\partial_t D(t)| dt + |\mathcal{M}(\tau_e)| - 1 \right], \quad (18)$$

where  $D(t) = D[\rho_1(t), \rho_2(t)] = |\mathcal{M}(t)|$  [79].

For different evolution time values, in Fig. 6 we depict the measure of non-Markovianity  $\mathcal{N}$  as a function of  $\lambda$  with  $\alpha = 0.4$  and  $N = 1000$  for two different values of

the evolution time. Comparing with the behavior of QSL time depicted in Fig. 5, one can clearly see that the qubit evolution slowdown at the critical point of the ESQPT is induced by the Markovian nature of the environment for short evolution times [Fig. 6(a)], whereas for longer evolution times, both  $\mathcal{N}$  and  $\tau_{\text{QSL}}$  exhibit a sharp peak at the critical point of the ESQPT [Fig. 6(b)]. In the latter case the quantum evolution slowdown phenomenon at the ESQPT critical point cannot be explained exclusively from the Markovian nature of the environment and we need to reexamine the mechanism of the evolution slowdown phenomenon at the critical point of ESQPT.

It is evident from Eq. (17) that the QSL time depends on the behavior of the decoherence rate of the qubit, i.e.,  $|\partial_t \mathcal{M}(t)|$ . Therefore, the evolution slowdown of the qubit at the critical point of the ESQPT can be explained from the singular behavior of the decoherence rate. To verify this conjecture, in the following of this section we study the dynamics of  $|\partial_t \mathcal{M}(t)|$ .

To this end, taking into consideration that the decoherence factor in Eq. (15) can be written as  $\mathcal{M}(t) = \sum_k e^{-iE_k t} |c_k|^2 = \int dE e^{-iEt} \omega(E)$ , where  $c_k = \langle k | \Psi_{\mathcal{E}, G}^0 \rangle$  denotes the expansion coefficient with  $|k\rangle$  of the  $k$ -th eigenstate of  $H_{\mathcal{E}}^{\frac{1}{2}}$  and  $E_k$  is the corresponding eigenenergy, while  $\omega(E) = \sum_k |c_k|^2 \delta(E - E_k)$ , denoted as strength function or local density of states [37], is the energy distribution of the initial state  $|\Psi_{\mathcal{E}, G}^0\rangle$  in the eigenstates of  $H_{\mathcal{E}}^{\frac{1}{2}}$ . Here, we should emphasize that the strength function  $\omega(E)$  shows a complex shape at the critical point of ESQPT, which leads to a singular behavior in the survival probability [26, 36–38]. Finally, we find that the expression of the decoherence rate can be written as

$$|\partial_t \mathcal{M}(t)| = \left| \int dE e^{-iEt} \mathcal{A}(E) \right|, \quad (19)$$

where

$$\mathcal{A}(E) = \sum_k |c_k|^2 E_k \delta(E - E_k). \quad (20)$$

Evidently,  $|\partial_t \mathcal{M}(t)|$  is the modulus of the Fourier transform of  $\mathcal{A}(E)$  and its time dependence can be easily obtained from  $\mathcal{A}(E)$ .

In Fig. 7, we display  $\mathcal{A}(E)$  and  $|\partial_t \mathcal{M}(t)|$  for different coupling strengths with  $\alpha = 0.4$  and  $N = 1000$ . Figs. 7(a)-(c) show  $\mathcal{A}(E)$  versus energy eigenvalues with coupling strength values below, at, and above the critical ones, respectively. We can see that for both non-critical coupling strengths  $\mathcal{A}(E)$  is unimodal [see Figs. 7(a) and 7(c)] and the peak location at  $\langle E \rangle = \sum_k |c_k|^2 E_k$  depends on the value of  $\lambda$ . Moreover, the width of  $\mathcal{A}(E)$  is approximately given by  $\text{Var}(E) = \sum_k |c_k|^2 E_k^2 - \langle E \rangle^2$ . However, the behavior of  $\mathcal{A}(E)$  at the critical coupling value is more complex [see Fig. 7(b)] with a double peak structure and negative (positive)  $\mathcal{A}(E)$  values for negative (positive) energies and, therefore  $\mathcal{A}(E_c) \approx 0$  at the ESQPT critical energy  $E_c = 0$ .

The time evolution of  $|\partial_t \mathcal{M}(t)|$  for the three coupling strengths discussed above is depicted in Figs. 7(d)-(f).

Firstly, we note that the time dependence of  $|\partial_t \mathcal{M}(t)|$  displays qualitatively similar patterns of regular damped oscillations for non-critical values of  $\lambda$  [see Figs. 7(d) and 7(f)]. These oscillations, depending on  $\langle E \rangle$  and on the fine structure of  $\mathcal{A}(E)$ , will have different frequencies and forms. Furthermore, the characteristic time of the decaying envelope can be connected to the width of  $\mathcal{A}(E)$  via a Heisenberg-like relation and the result is given by  $\tau_c \propto 1/\text{Var}(E)$ . Secondly, a different pattern for  $|\partial_t \mathcal{M}(t)|$ , characterized by irregular oscillations, can be clearly appreciated at the critical coupling [see Fig. 7(e)]. The regular damped recurrences displayed in Figs. 7(d) and 7(f) are replaced by an initial sharp increase followed by groups of random oscillations. Notice the different  $y$ -axis scaling in Figs. 7(e-f), with  $|\partial_t \mathcal{M}(t)|$  attaining minimum values for  $\lambda = \lambda_c$ . The behavior of  $|\partial_t \mathcal{M}(t)|$  at the critical point of the ESQPT can be traced back to the particular form of  $\mathcal{A}(E)$  shown in Fig. 7(b).

In summary, we have shown that the existence of an ESQPT in the spectrum of the environment has a strong influence on the dynamics of the qubit as can be seen from the time dependence of  $|\partial_t \mathcal{M}(t)|$ . At the critical value of the coupling strength, which leads the environment to the ESQPT critical energy,  $|\partial_t \mathcal{M}(t)|$  displays a random oscillatory pattern of small amplitude. *Therefore, the aforementioned conjecture is strongly supported by the singular behavior of  $|\partial_t \mathcal{M}(t)|$ .*

## V. CONCLUSIONS

In conclusion, we have analyzed the effects of an ESQPT on the QSL of an open quantum system by studying a central qubit coupled to a spin environment modeled by a LMG bath. The signatures of the ESQPT in the environment are either a divergence of the second order derivative of an individual excite state energy with respect to the control parameter, or a singularity in the local density of states at the critical energy ( $E_c = 0$ ) for a constant control parameter. By quenching the coupling strength between the qubit and the environment, we have

probed the impact that the ESQPT in the environment has upon the QSL time of the qubit.

We have found that the environment underlying ESQPT produces conspicuous effects in the QSL time of the qubit. Namely, the QSL time of the qubit displays a sharp peak at the critical point of the ESQPT, making the ESQPT responsible for a noticeable slow down in the qubit evolution. Moreover, at the critical point of the ESQPT, the QSL time approach the actual evolution time value for increasing environment size. In spite of the fact that long evolution times are associated with small values of the QSL time of the qubit, the maximum of the QSL time is always located at the critical energy of the ESQPT making the QSL time as a viable proxy for assessing the existence of an ESQPT in the environment.

With a calculation of a non-Markovianity measure for the open system under consideration, we have demonstrated that the qubit evolution slowdown at the critical point of ESQPT cannot be always explained from the Markovian nature of the environment. In fact, the particular behavior of the QSL time at the critical point of the ESQPT stems from the singular behavior of  $|\partial_t \mathcal{M}(t)|$ . Our work, therefore, provide an additions to previous works that investigate the relation between the QSL and the Markovian character of the environment (see, e.g., Ref. [46] and references therein).

The results reported in this work advance an original point of view of the influence of ESQPTs on quantum system dynamics. Furthermore, considering the recent experimental progresses on the detection of ESQPT signatures [32–35], the QSL can be considered of an experimental proxy for ESQPTs in the laboratory.

## ACKNOWLEDGMENTS

FPB contribution to this work was partially funded by MINECO grant FIS2014-53448-C2-2-P and by the CEAFMC at the Universidad de Huelva. The authors would like to thank Lea Santos for useful discussions and suggestions.

- 
- [1] L. Carr, *Understanding quantum phase transitions*, Condensed Matter Physics (Taylor and Francis, Hoboken, NJ, 2010).
  - [2] S. Sachdev, *Quantum Phase Transitions* (Cambridge University Press, Cambridge, 2011).
  - [3] A. Dutta, G. Aeppli, B. K. Chakrabarti, U. Divakaran, T. F. Rosenbaum, and D. Sen, *Quantum Phase Transitions in Transverse Field Spin Models: From Statistical Physics to Quantum Information* (Cambridge University Press, Cambridge, 2015).
  - [4] C. Emary and T. Brandes, Phys. Rev. E **67**, 066203 (2003).
  - [5] W. H. Zurek, U. Dorner, and P. Zoller, Phys. Rev. Lett. **95**, 105701 (2005).
  - [6] H. T. Quan, Z. Song, X. F. Liu, P. Zanardi, and C. P. Sun, Phys. Rev. Lett. **96**, 140604 (2006).
  - [7] A. Silva, Phys. Rev. Lett. **101**, 120603 (2008).
  - [8] J. Dziarmaga, Adv. Phys. **59**, 1063 (2010).
  - [9] A. Polkovnikov, K. Sengupta, A. Silva, and M. Vengalattore, Rev. Mod. Phys. **83**, 863 (2011).
  - [10] M. Greiner, O. Mandel, T. Esslinger, T. Hansch, and I. Bloch, Nature **415**, 39 (2002).
  - [11] I. Bloch, J. Dalibard, and W. Zwerger, Rev. Mod. Phys. **80**, 885 (2008).
  - [12] K. Baumann, C. Guerlin, F. Brennecke, and T. Esslinger, Nature **464**, 1301 (2010).
  - [13] R. Gilmore, J. Math. Phys. **20**, 891 (1979).

- [14] D. H. Feng, R. Gilmore, and S. R. Deans, Phys. Rev. C **23**, 1254 (1981).
- [15] F. Iachello and N. V. Zamfir, Phys. Rev. Lett. **92**, 212501 (2004).
- [16] P. Cejnar and F. Iachello, Journal of Physics A: Mathematical and Theoretical **40**, 581 (2007).
- [17] P. Cejnar, J. Jolie, and R. F. Casten, Rev. Mod. Phys. **82**, 2155 (2010).
- [18] P. Cejnar, M. Macek, S. Heinze, J. Jolie, and J. Dobe, J. Phys. A: Math. and Gen. **39**, L515 (2006).
- [19] P. Cejnar and P. Stránský, Phys. Rev. E **78**, 031130 (2008).
- [20] M. Caprio, P. Cejnar, and F. Iachello, Ann. Phys. **323**, 1106 (2008).
- [21] F. Leyvraz and W. D. Heiss, Phys. Rev. Lett. **95**, 050402 (2005).
- [22] P. Pérez-Fernández, A. Relaño, J. M. Arias, J. Dukelsky, and J. E. García-Ramos, Phys. Rev. A **80**, 032111 (2009).
- [23] P. Stránský, M. Macek, and P. Cejnar, Ann. Phys. **345**, 73 (2014).
- [24] A. Relaño, J. M. Arias, J. Dukelsky, J. E. García-Ramos, and P. Pérez-Fernández, Phys. Rev. A **78**, 060102 (2008).
- [25] F. Pérez-Bernal and F. Iachello, Phys. Rev. A **77**, 032115 (2008).
- [26] P. Pérez-Fernández, P. Cejnar, J. M. Arias, J. Dukelsky, J. E. García-Ramos, and A. Relaño, Phys. Rev. A **83**, 033802 (2011).
- [27] P. Cejnar and J. Jolie, Progr. Part. Nucl. Phys. **62**, 210 (2009).
- [28] V. M. Bastidas, P. Pérez-Fernández, M. Vogl, and T. Brandes, Phys. Rev. Lett. **112**, 140408 (2014).
- [29] P. Pérez-Fernández, A. Relaño, J. M. Arias, P. Cejnar, J. Dukelsky, and J. E. García-Ramos, Phys. Rev. E **83**, 046208 (2011).
- [30] T. Brandes, Phys. Rev. E **88**, 032133 (2013).
- [31] M. Kloc, P. Strnsk, and P. Cejnar, Annals of Physics **382**, 85 (2017).
- [32] B. Dietz, F. Iachello, M. Miski-Oglu, N. Pietralla, A. Richter, L. von Smekal, and J. Wambach, Phys. Rev. B **88**, 104101 (2013).
- [33] D. Larese and F. Iachello, J. Molec. Struct. **1006**, 611 (2011).
- [34] D. Larese, F. Pérez-Bernal, and F. Iachello, J. Molec. Struct. **1051**, 310 (2013).
- [35] L. Zhao, J. Jiang, T. Tang, M. Webb, and Y. Liu, Phys. Rev. A **89**, 023608 (2014).
- [36] L. F. Santos and F. Pérez-Bernal, Phys. Rev. A **92**, 050101 (2015).
- [37] L. F. Santos, M. Távora, and F. Pérez-Bernal, Phys. Rev. A **94**, 012113 (2016).
- [38] F. Pérez-Bernal and L. F. Santos, Progr. Phys. Fortschr. Phys. **65**, 1600035 (2017).
- [39] Q. Wang and H. T. Quan, Phys. Rev. E **96**, 032142 (2017).
- [40] G. Engelhardt, V. M. Bastidas, W. Kopylov, and T. Brandes, Phys. Rev. A **91**, 013631 (2015).
- [41] R. Puebla, A. Relaño, and J. Retamosa, Phys. Rev. A **87**, 023819 (2013).
- [42] R. Puebla and A. Relaño, Phys. Rev. E **92**, 012101 (2015).
- [43] M. Kloc, P. Stránský, and P. Cejnar, Phys. Rev. A **98**, 013836 (2018).
- [44] W. Kopylov, G. Schaller, and T. Brandes, Phys. Rev. E **96**, 012153 (2017).
- [45] P. Pérez-Fernández and A. Relaño, Phys. Rev. E **96**, 012121 (2017).
- [46] S. Deffner and S. Campbell, Phys. A: Math. and Theor. **50**, 453001 (2017).
- [47] M. R. Frey, Quantum Inf. Process. **15**, 3919 (2016).
- [48] S. Deffner and E. Lutz, Phys. Rev. Lett. **111**, 010402 (2013).
- [49] M. M. Taddei, B. M. Escher, L. Davidovich, and R. L. de Matos Filho, Phys. Rev. Lett. **110**, 050402 (2013).
- [50] A. del Campo, I. L. Egusquiza, M. B. Plenio, and S. F. Huelga, Phys. Rev. Lett. **110**, 050403 (2013).
- [51] Y.-J. Zhang, W. Han, Y.-J. Xia, J.-P. Cao, and H. Fan, Sci. Rep. **4** (2014), 10.1038/srep04890.
- [52] Z. Sun, J. Liu, J. Ma, and X. Wang, Sci. Rep. **5** (2015), 10.1038/srep08444.
- [53] H.-B. Liu, W. L. Yang, J.-H. An, and Z.-Y. Xu, Phys. Rev. A **93**, 020105 (2016).
- [54] I. Marvian, R. W. Spekkens, and P. Zanardi, Phys. Rev. A **93**, 052331 (2016).
- [55] A. Ektesabi, N. Behzadi, and E. Faizi, Phys. Rev. A **95**, 022115 (2017).
- [56] X. Cai and Y. Zheng, Phys. Rev. A **95**, 052104 (2017).
- [57] D. C. Brody, J. Phys. A: Math. and Gen. **36**, 5587 (2003).
- [58] B. Shanahan, A. Chenu, N. Margolus, and A. del Campo, Phys. Rev. Lett. **120**, 070401 (2018).
- [59] M. Okuyama and M. Ohzeki, Phys. Rev. Lett. **120**, 070402 (2018).
- [60] Y.-B. Wei, J. Zou, Z.-M. Wang, and B. Shao, Sci. Rep. **6**, 19308 (2016).
- [61] L. Hou, B. Shao, and J. Zou, Eur. Phys. J. D **70**, 35 (2016).
- [62] H. J. Lipkin, N. Meshkov, and A. J. Glick, Nucl. Phys. **62**, 188 (1965).
- [63] F. M. Cucchietti, S. Fernandez-Vidal, and J. P. Paz, Phys. Rev. A **75**, 032337 (2007).
- [64] M. Šindelka, L. F. Santos, and N. Moiseyev, Phys. Rev. A **95**, 010103 (2017).
- [65] T. Monz, P. Schindler, J. T. Barreiro, M. Chwalla, D. Nigg, W. A. Coish, M. Harlander, W. Hänsel, M. Hennrich, and R. Blatt, Phys. Rev. Lett. **106**, 130506 (2011).
- [66] C. Gross, T. Zibold, E. Nicklas, J. Estve, and M. K. Oberthaler, Nature **464**, 1165 (2010).
- [67] M. F. Riedel, P. Bhi, Y. Li, T. W. Hnsch, A. Sinatra, and P. Treutlein, Nature **464**, 1170 (2010).
- [68] I. D. Leroux, M. H. Schleier-Smith, and V. Vuletić, Phys. Rev. Lett. **104**, 073602 (2010).
- [69] A. Frank and P. V. Isacker, *Algebraic Methods in Molecular and Nuclear Structure Physics* (John Wiley and Sons, New York, 1994).
- [70] P. Ribeiro, J. Vidal, and R. Mosseri, Phys. Rev. E **78**, 021106 (2008).
- [71] M. C. Gutzwiller, *Chaos in Classical and Quantum Mechanics* (Springer-Verlag, Berlin, 1990).
- [72] W. D. Heiss and M. Müller, Phys. Rev. E **66**, 016217 (2002).
- [73] T. Gorin, T. Prosen, T. H. Seligman, and M. nidari, Phys. Rep. **435**, 33 (2006).
- [74] H. P. Breuer and F. Petruccione, *The theory of Open Quantum Systems* (Oxford University Press, Oxford, 2007).

- [75] Z.-Y. Xu, S. Luo, W. L. Yang, C. Liu, and S. Zhu, Phys. Rev. A **89**, 012307 (2014).
- [76] A. D. Cimmarusti, Z. Yan, B. D. Patterson, L. P. Corcos, L. A. Orozco, and S. Deffner, Phys. Rev. Lett. **114**, 233602 (2015).
- [77] H.-P. Breuer, E.-M. Laine, and J. Piilo, Phys. Rev. Lett. **103**, 210401 (2009).
- [78] S. Wißmann, A. Karlsson, E.-M. Laine, J. Piilo, and H.-P. Breuer, Phys. Rev. A **86**, 062108 (2012).
- [79] P. Haikka, J. Goold, S. McEndoo, F. Plastina, and S. Maniscalco, Phys. Rev. A **85**, 060101 (2012).